POAC '99
Espoo, Finland

Proceedings of the 15th
International Conference on
Port and Ocean Engineering
under Arctic Conditions

NUMERICAL SIMULATION OF SEA ICE DRIFT IN THE BAY OF BOTHNIA

Z.H. Zhang, M. Leppäranta, J.J. Haapala and T. Stipa
Department of Geophysics, P.O. Box 4 (Fabianinkatu 24 A),
FIN-00014 University of Helsinki, Finland

ABSTRACT

Sea ice drift in the coastal ice zone of the Bay of Bothnia was measured with five GPS drifters in March 1997. To model coastal ice dynamics, the viscous-plastic ice model of Hibler with a fine spatial resolution of 5 km is used. A truncated elliptical yield curve is used preventing any tensile stress from occurring. Thermodynamics are neglected because our interest is in ice dynamics. The model simulation is run for 20 days, which covers the whole experiment period. The results show that the observed characteristics of the pack ice motion can be realistically simulated by the model. The ice drift trajectories obtained from the model demonstrate good agreement with drifter data in most of the period. Comparison of modeled ice displacements with sequential SAR data on the basin wide scale is also made and the agreement is in general quite good. The ice field in the coastal ice zone illustrated strong rigid and plastic patterns, suggesting an ice strength constant $P^*=3.0\times10^4$ N/m^2 being best representative.

1. INTRODUCTION

Sea ice motion is mainly wind driven in the Baltic Sea. Solid boundary (coastline or fast ice boundary) highly influences the ice motion and thickness redistribution. The internal ice stress, depending on the ice conditions and the boundary geometry, is an important factor and has the same order of magnitude as the wind stress. An early study of Leppäranta (1981) indicated that the fast ice boundary causes heavy ice deformation in the Bay of Bothnia. The solid boundary, on the other hand, causes open water formation when the ice moves away from it. Therefore, large spatial and temporal variations in ice velocity and thickness redistribution occur through the generation of leads and deformed ice.

A sea ice experiment ZIP-97 (Zooming of Ice Physics), a part of the project "Local Ice Cover Deformation and Mesoscale Ice Dynamics" or ICE STATE, has been carried out in the Baltic Sea in March 1997. ZIP-97 offered the first opportunity to study sea ice drift and deformation with GPS drifter array in the Baltic Sea. The drifter data is an important part of ZIP-97 and is a link between the basin scale ice dynamics and the local scale deformations; one of the main objectives of the ICE STATE project is to study connections between different scales in ice dynamics. Five drifters were deployed in the Bay of Bothnia on 10-20 kilometers spatial scale.

A dynamic sea ice model is used to simulate ice dynamics in the ZIP-97 case. The model is based on Hibler (1979) viscous-plastic ice model. However, many new features have been added. In addition to elliptical yield curve, a more realistic truncated elliptical yield curve is chosen. An efficient numerical method for solving momentum balance proposed by Zhang and Hibler (1997) is used instead of the old procedure of Hibler (1979), and a moving

ice/water boundary has been taken account. To realistically simulate ice motion near the coasts, a no-slip/free boundary condition is proposed in the present work. The present paper shows preliminary model results and comparisons with observed data. The goal is to examine how well a continuum model can reproduce ice motion on the fine scale of 5 km.

2. MODEL DESCRIPTION

The present model is based on Hibler's (1979) viscous-plastic ice model. The momentum balance equation involves the inertial term, Coriolis force, air stress, water stress and internal ice stress. The mass conservation is described by two-level ice thickness distribution equations. Thermodynamics are not included because our interests are the dynamic process of sea ice. This is a good approximation for the first half of the study period but may slightly underestimate the rigidity of the ice in the second half. The air and water stresses are parameterized by the well-known quadratic drag laws. The air drag coefficient is 1.8×10^{-3} (Haapala and Leppäranta, 1996) and the turning angle is zero because the surface wind is used. The ocean current field beneath the frictional surface layer is assumed equal to zero, and the corresponding ice/water drag coefficient is $C_w = 3.5\times10^{-3}$ and turning angle θ =18° (Leppäranta, 1990). Again this is a source of some inaccuracy; but anyway the main forces in the ice dynamics were the wind stress and internal friction of ice in the study case. The internal ice stress tensor is obtained using the nonlinear viscous-plastic constitutive rheology of Hibler (1979)

$$\sigma = 2\eta\dot{\varepsilon} + (\zeta - \eta)tr\dot{\varepsilon}\boldsymbol{I} - P\boldsymbol{I}/2, \tag{1}$$

$$\zeta = P/2\Delta,\ \eta = \zeta/e^2, \tag{2a,b}$$

$$\Delta = [(\dot{\varepsilon}_1 + \dot{\varepsilon}_2)^2 + (\dot{\varepsilon}_1 - \dot{\varepsilon}_2)^2/e^2)]^{1/2} \tag{3}$$

where $\dot{\varepsilon}$ is strain rate tensor, $\boldsymbol{I}$ is the unit tensor, ζ and η are nonlinear bulk and shear viscosities, e is the aspect ratio of the yield curve, $\dot{\varepsilon}_1$ and $\dot{\varepsilon}_2$ are the principal strain rates, and P is the ice strength expressed by

$$P = P^* h \exp(-C(1-A)), \tag{4}$$

where P^* is the ice strength constant and C is the strength reduction constant for opening, h is mean ice thickness and A is ice compactness.

To avoid occurrence of arbitrarily large of ζ and η for very small strain rates, Δ is bounded below by $\dot{\varepsilon}_0$, where $\dot{\varepsilon}_0$ is maximum rate of viscous creep that describes how easily the stress state can reach the yield curve. When $\Delta > \dot{\varepsilon}_0$, the ice moves as a plastic fluid, otherwise it moves as a linear viscous fluid. To well approximate plastic behavior, the creep limit $\dot{\varepsilon}_0$ has to be small enough. In the present simulation, we set $\dot{\varepsilon}_0 = 10^{-10}\mathrm{s}^{-1}$ which is less by 2-3 order of magnitude than the measurement accuracy.

The yield curve described by equation (1) is an ellipse in principal stresses space, and its size and shape are specified by P and e. However, use of this yield curve and normal flow rule

leads to unphysical effects (tensile strength >0) whenever the stress state lies in the fourth (or the second) quadrant. To avoid this, we follow the idea described by Hibler and Schulson (1997) to prevent any tensile stress from occurring in such a way that

$$\sigma_1 = 0 \tag{5}$$

whenever σ_1 is positive. Note we have assumed $\sigma_2 \le \sigma_1$, where σ_1 and σ_2 are the principal stress components of the stress tensor σ

$$\sigma_{1,2} = \zeta(\dot{\varepsilon}_1 + \dot{\varepsilon}_2) + \eta(\dot{\varepsilon}_1 - \dot{\varepsilon}_2) - P/2 . \tag{6a,b}$$

If we define η such that

$$\eta = \frac{P/2 - \zeta(\dot{\varepsilon}_1 + \dot{\varepsilon}_2)}{|(\dot{\varepsilon}_1 - \dot{\varepsilon}_2)|}, \tag{7}$$

then the condition (5) will always be satisfied.

Thus the yield curve in the present model is an elliptical truncated yield curve (see Fig. 1). It describes a rheology with no tensile stress and the shear stress under divergent conditions is substantially reduced compared with the conventional elliptical yield curve.

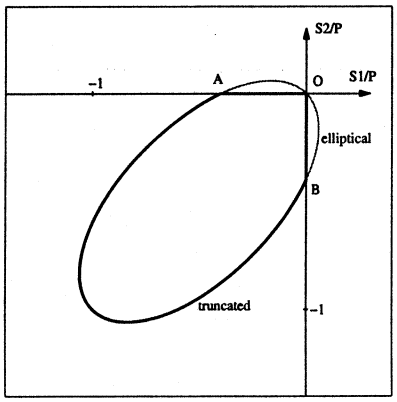

Figure 1. Elliptical yield curves in normalized principal stresses space (S1 and S2 are the principal stresses). Bold curve OABO defines the elliptical truncated yield curve.

To simulate GPS drifter trajectories, model grid size should be able to distinguish different drifters. In the present case the grid size is 5 km that is half of size normally used in the Baltic Sea (Haapala and Leppäranta, 1996). We expect that this grid size does not severely violate the continuum approximation in the Hibler model, it is, in fact, still one order of magnitude large than typical ice floe size. The time step is 15 minutes. The model boundaries consist of both solid boundary and ice/water moving boundary. Because the drifter locations in our case were very close to the land fast ice boundary, formulation of the boundary condition on the solid boundary is crucial in the simulation. On the solid boundary the ice velocity is set to zero when ice moves toward the boundary, otherwise it is equal to the mean

value of adjacent internal points. An analogous treatment is adopted for the ice/water boundary. The ice velocity is set equal to the mean value of adjacent internal points when the velocity is directed toward interior, otherwise it is equal to the free-drift velocity. Thus, the ice/water boundary is assumed to be of a stress-free type.

3. RESULTS

3.1 Weather and ice conditions

The weather and ice conditions during the experiment period are shown in Figs 2-3. We see that the weather conditions can be divided into two periods. In the first period (3-13 March) the weather was warm and the air temperature was around 0°C. Southwesterly and westerly winds prevailed with several strong storms on 5, 9 and 13 March. The thickness distribution of the ice illustrated large variability in time and space due to the wind stress forcing. The level ice thickness on 3 March was typically 30-50 cm in the eastern part of the bay and decreased westward to 10-30 cm near the ice edge. There were heavy ridged and rafted areas along the eastern fast ice edge. In the next five days the ice field was further consolidated and the ice cover area decreased due to strong winds. In the second period, after 14 March, cold northerly winds were dominated and the temperature consequently dropped down between -5° to -15°C. The ice cover was driven southwestward by the wind, forming open leads in the north part of the bay. A large area of pack ice was separated from the heavily consolidated ice zone in the eastern part (see the ice map 20.3 in Fig. 3). As the ice dispersed, the sea surface was exposed to the air. The thermal heat budget and the force balance were changed and new ice formed in the north. The Bay of Bothnia was again totally ice covered around 24 March.

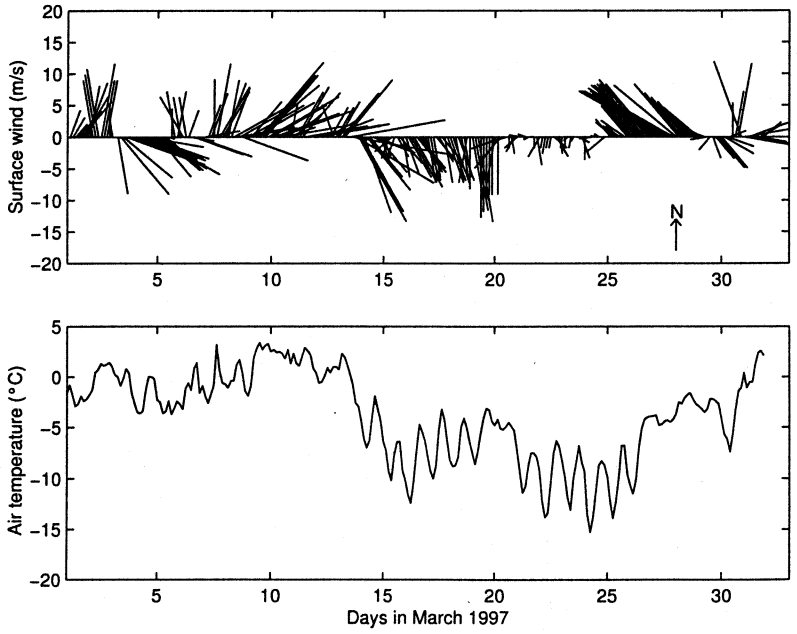

Figure 2. Wind and air temperature in March 1997 at Kemi-1 station (24°06 E, 65°23 N, 26 meters above sea level).

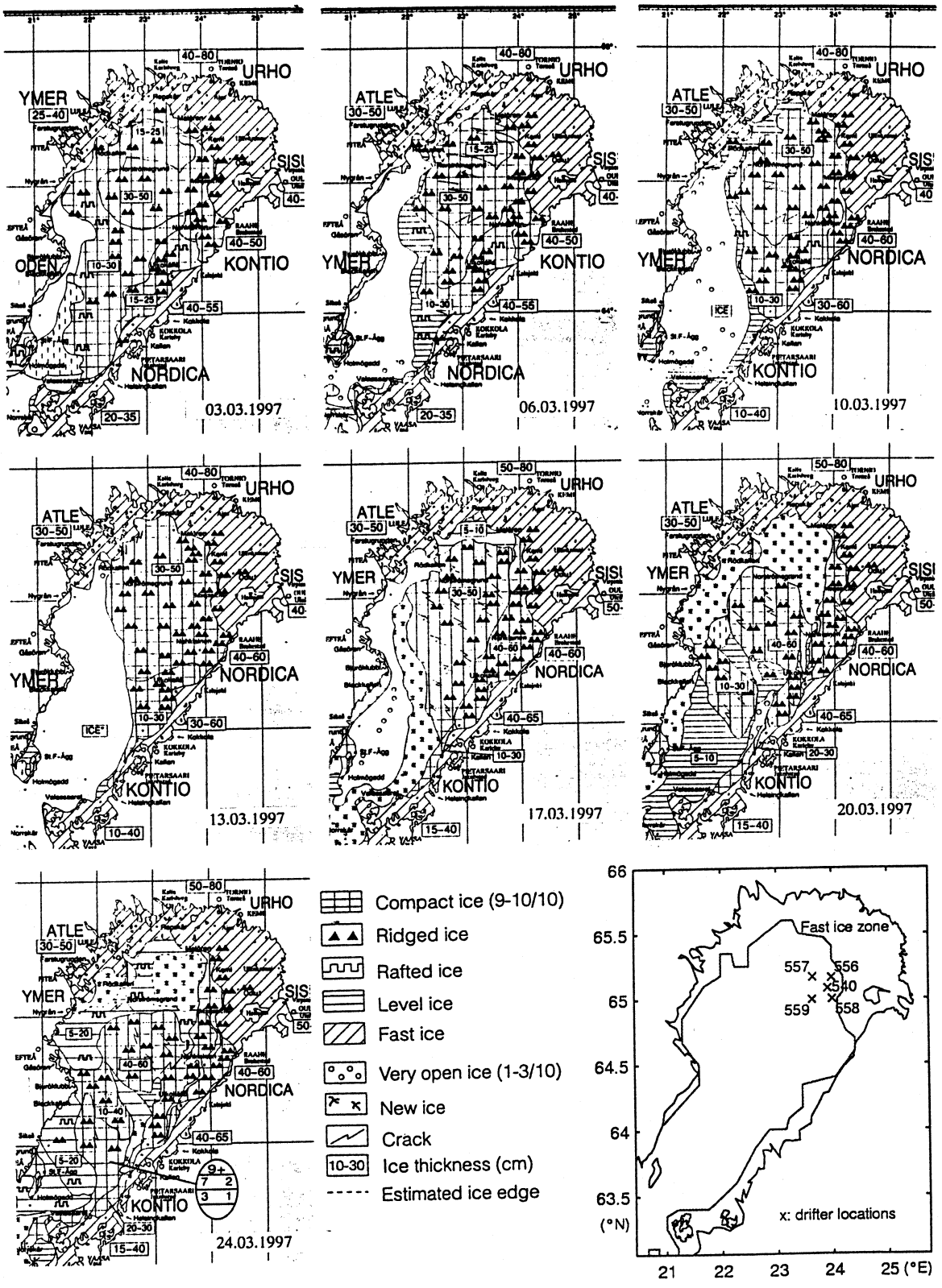

Figure 3. Observed ice conditions in March 1997. The cross marks in the right lower figure are the initial positions of GPS drifters.

3.2 Initial condition, wind forcing data and model parameters

The input of the model consists of ice thickness, compactness and wind stress. The initial ice thickness and compactness were obtained from the FIMR ice chart of 3 March. The typical level ice thickness was 30-50 cm in the eastern part and 10-30 cm in the west and south parts. The compactness was more than 90% over the most ice covered area. Near the ice edge and southern part of the bay the compactness was 50-80%. The wind forcing data came from the Finnish Meteorological Institute (FMI) station data (Kemi-1, Marjanieni and Ulkokalla) and the Swedish Meteorological and Hydrological Institute (SMHI) geostrophic wind data of 1°x1° grid. The station wind data were adjusted to winds measured at the standard 10-m anemometer height (Fissel and Tang, 1991). The speed ratio and tuning angle between geostrophic wind and surface wind are 0.6 and 34°, respectively (Bumer *et al.*, 1998). These wind data have 3 hours time interval. They were first spatially interpolated into the ice model grid by a simple objective analysis procedure and then linearly interpolated for 1 hour time intervals. The simulation was performed for 20 days (3-23 March), which covers the whole experiment period. Ice rheology parameters used in the model are $P^*=3.0\times10^4$ Nm^{-2}, e=2.0, C=20 and $\dot{\varepsilon}_0 = 10^{-10}\text{s}^{-1}$.

3.3 Comparison of model results and drifter data

Five drifters were deployed on the drift pack ice zone by a helicopter during 5-7 March. The initial geometry of the drifter locations (see Figure 3) formed a square with four drifters at each corner (NE-556, NW-557, SE-558 and SW-559) and one at the center (CE-540). The side of the square was about 18 km. The observed and simulated ice drift trajectories for the periods of data being available are shown in Fig. 4.

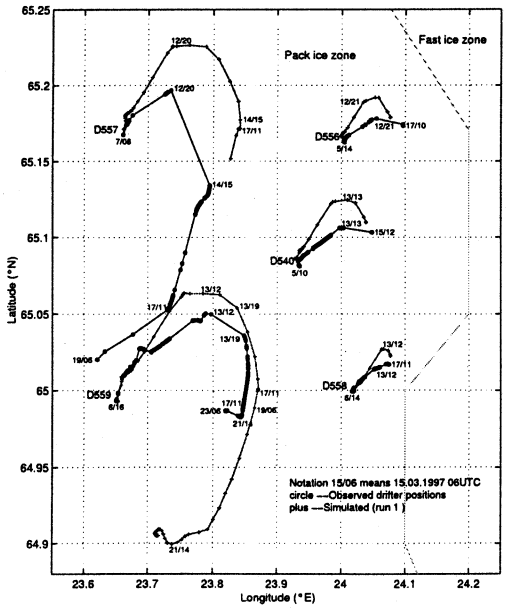

Figure 4. Observed (circle marks) and simulated (plus marks) GPS drifter trajectories during the experiment period.

It can be seen that all drifters traveled first northeastward during the first period. Owing to high compression within the ice pack, the ice cover moved very slowly and the displacements were only a few kilometers for the eastern drifters (556, 558 and 540) and about 6 and 9 km for the western drifters (557 and 559). The drifter 556 and 540 stopped working on 12 and 13 March, respectively, due to severe ice conditions. A visual comparison between model results and observed data indicates that the agreement is quite good for all drifters during this period.

In the second period, the wind direction was changed and northerly winds prevailed. The eastern drifters were almost stationary with only small displacements (drifter 556 and 540 were found by helicopter about 2 km eastward away from their last positions on 15 and 17 March, respectively). Drifter 559 also moved slowly with a southward displacement about 7 km. Drifter 557, however, displayed large mobility, which was significantly different from the other four. It traveled about 15 km southwestward during 14-19 March. The model results still show good agreement for drifters 540, 556, 558 and 559 (before 19 March). However, large discrepancies are found at drifter 559 after 19 March for which the model results illustrate larger displacements than the observed data. Large discrepancies are also found for drifter 557 during the period 14-19 March for which the observed large displacement cannot be reproduced by the model.

A synchronous comparison of ice deformation polygons is shown in Fig. 5. We see that the main discrepancies between model results and observed data are from drifter 557. A possible reason is that there existed large open leads between drifter 557 and other four during 14-19 March, resulting in large deformation in the real ice field that was not simulated by the model.

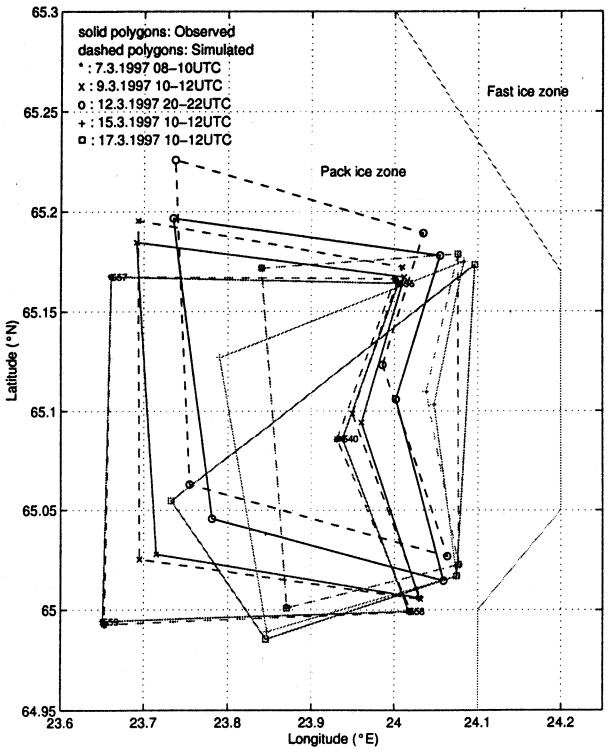

Figure 5. Observed (solid lines) and simulated (dashed lines) drifter deformation polygons during the experiment period.

3.4 Comparison of model results and observed data in the basin scale

Comparison with sequential SAR data on the basin wide scale has been also made and is illustrated in Fig. 6. The model results show good agreement in the coastal ice zone. Note, the displacements from the model are in closer agreement with the drifter data than with the displacements in the SAR data for the period 12-15 March. There are large discrepancies out of the coastal ice zone. The magnitude of model displacements is only about half of SAR data. The possible sources of these discrepancies can be produced by factors related to both the model and the data, for instance, incomplete physics of the model, uncertainty of the model parameters and errors from the SAR data.

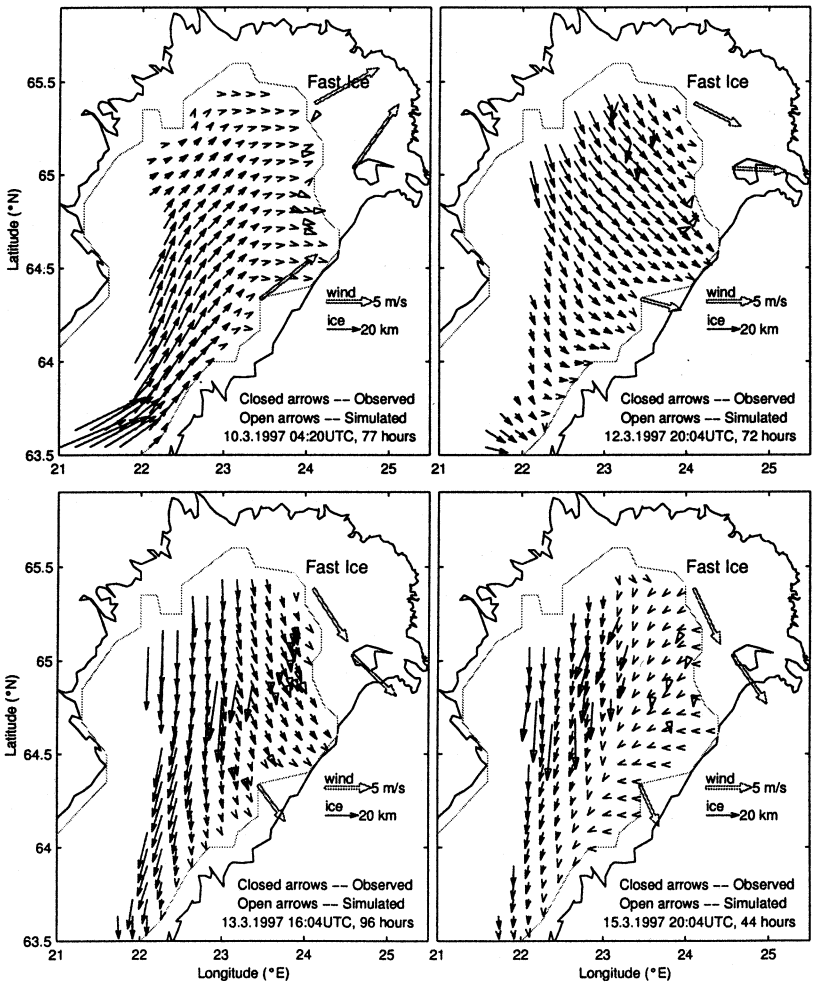

Figure 6. Comparison of ice displacements between model results and SAR data. The SAR displacement data are obtained from NERSC (Sandven et.al., 1997).

The modeled ice thickness fields on March 6, 10, 13 and 20 are illustrated in Fig. 7. Compared with Fig. 3, we see that the thickness redistribution in the real ice fields showed large variability in time and space. The heavy ridge buildup formed along the Finnish coastline and the large opening areas formed in the west and north sides during the experiment period. These can be fairly well reproduced by the model and the overall agreement is good.

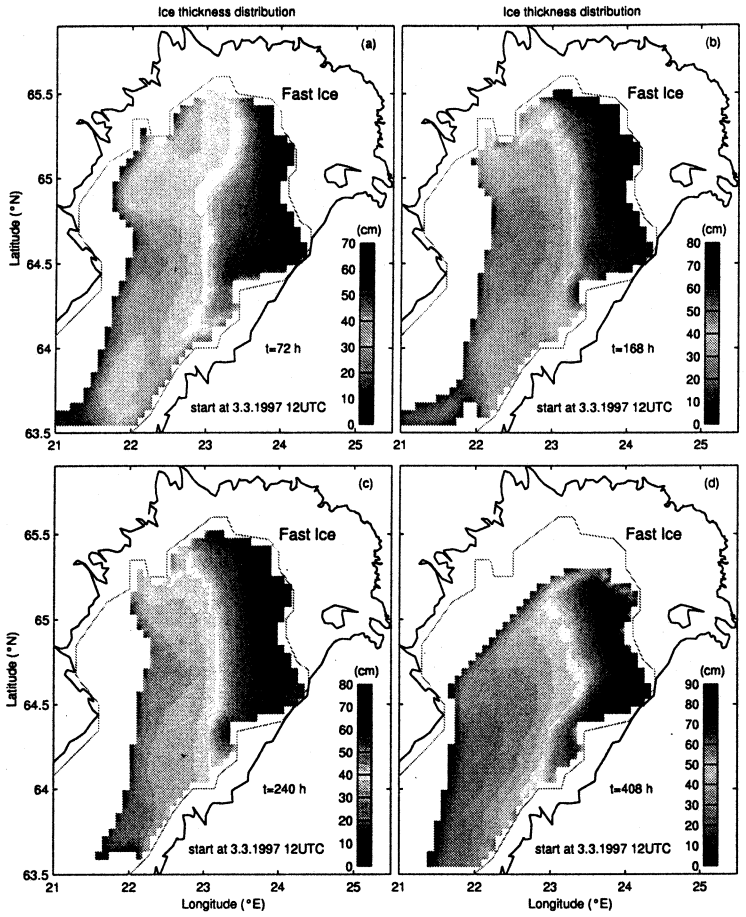

Figure 7. Modeled thickness distributions on March 6, 10,13, 20 (notated by 72, 168, 240 and 408 hours), respectively.

4. CONCLUSIONS

We have developed a high spatial resolution (5 km grid size) dynamic sea ice model capable of applying for coastal seas. The model is based on Hibler (1979) viscous-plastic model. A truncated elliptical yield curve that can prevent occurrence of any tensile stress is used. An efficient numerical method for solving momentum balance (Zhang and Hibler, 1997) is employed. A simulation for ice drift observations in the Bay of Bothnia was made. The results show that the present model is able to produce a realistic simulation of the observed ice motion and the overall agreement is very encouraging. This indicates that it is possible to reduce model grid size to 5 km for the Baltic Sea without severely violating the continuum approximation in the Hibler model. The ice field demonstrated strong rigid and plastic features and the value of ice strength constant $P^*=3.0\times10^4$ Nm^{-2} is a suitable value for this case. Comparison with SAR displacement data shows that the agreement in the coastal ice zone is good, but there are large discrepancies near the ice edge.

The sources of discrepancies between model results and observed data can be accounted for factors related to both the model and the data. These include incomplete physics of the model, uncertainty of the model parameters and errors of the data. The present model is an

isotropic model, which is not able to simulate anisotropic behavior that is often observed in real ice fields. The model parameters (drag coefficients and rheology parameters) used in the model simulation are constant. These values, as illustrated by Leppäranta *et al.* (1998), may be different in time and space in the Baltic Sea. The wind forcing data used in the simulation have an interval of three hours and hence are unable to reproduce ice motion under conditions of rapidly varying wind field. Furthermore, errors in the initial ice fields, lack of an ocean model in providing realistic water currents, and influence of ice thermodynamics may also be causes of the discrepancies.

Although the present model provides satisfactory results of ice drift, further improvements are still needed. An anisotropic model, which could generate open leads, is worthwhile developing and more complex rheology should be considered. Problems such as these require a very careful study of physical basis for relation between stress and strain-rate, which is expected to be possible with the help of more accurate and detailed observations.

Acknowledgments: Authors would like to thank Dr. Jinlun Zhang for providing model code of the efficient numerical method for solving momentum balance. This work is part of the project Local Cover Deformation and Mesoscale Ice Dynamics or ICE STATE supported by the European Commission, DG XII, through the Marine Science and Technology programme 1994-1998 (MAST III) under contract MAS3-0006. The participants in the joint project are Helsinki University of Technology, Nansen Environment and Remote Sensing Center, Scott Polar Research Institute, University of Helsinki, and University of Iceland.

REFERENCES

Bumer, K., Karger, U., Hasse, L. and Niekamp, K. 1998. Evaporation over the Baltic Sea as an example of a seme-enclosed sea. *Contr. Atmos. Phys.*, **71**, 249-261.

Fissel, D.B. and Tang, C.L. 1991. Response of sea ice drift to wind forcing on the Northeastern Newfoundland Shelf. *J. Geophys. Res.*, **96**, 18397-18409.

Haapala, J. and Leppäranta, M. 1996. Simulations of the ice season in the Baltic Sea. *Tellus*, **48A**, 622-643.

Leppäranta, M., Sun, Y. and Haapala, J. 1998. Comparisons of sea-ice velocity fields from ERS-1 SAR and a dynamic model. *J. Glaciology*, **147**, 248-261.

Hibler III, W.D. 1979. A dynamic and thermodynamic sea ice model. *J. Phys. Oceanogr.*, **9**, 815-846.

Hibler III, W.D. and Schulson, E.M. 1997. On modeling sea-ice fracture and flow in numerical investigations of climate. *Annals of Glaciology*, **25**, 26-32.

Leppäranta, M. 1981. On the structure and mechanics of pack ice in the Bothnian Bay. *Finnish Mar. Res.*, **248,** 3-86.

Leppäranta, M. 1990. Observations of free drift ice drift and currents in the Bay of Bothnia. *Göteborg Kungliga Vetenskaps-och Vitterhets-Samhället Acta, Ser. Geofys.* **3**, 84-97.

Sandven, S., Alexandrov, V., Lundhaug, M., Kloster, K., Hamre, T. and Dalen, O. 1997. Satellite remote sensing of sea ice in the Bothnian Bay during March 1997. *NERSC Technical Report* **No. 130**, 66p.

Zhang, J. and Hibler III, W.D. 1997. On an efficient numerical method for modeling sea ice dynamics. *J. Geophys. Res.*, **102**, 8691-8702.